Dalton Transactions

IPr*^{Oxa} – A New Class of Sterically-Hindered, Wingtip-Flexible N,C-Chelating Oxazole-Donor N-Heterocyclic Carbene Ligands

Journal:	*Dalton Transactions*
Manuscript ID	DT-ART-07-2023-002255.R1
Article Type:	Paper
Date Submitted by the Author:	23-Aug-2023
Complete List of Authors:	Podchorodecka, Pamela; Opole University, Department of Chemistry Dziuk, Błażej; Wroclaw University of Science and Technology, Faculty of Chemistry Szostak, Roman; University of Wroclaw, Chemistry Szostak, Michal; Rutgers University, Department of Chemistry Bisz, Elwira; Opole University, Department of Chemistry

PAPER

IPr*^{Oxa} – A New Class of Sterically-Hindered, Wingtip-Flexible N,C-Chelating Oxazole-Donor N-Heterocyclic Carbene Ligands

Pamela Podchorodecka,[a] Błażej Dziuk,[b] Roman Szostak,[c] Michal Szostak*,[d] and Elwira Bisz*,[a]

Received 00th January 20xx,
Accepted 00th January 20xx

DOI: 10.1039/x0xx00000x

N-Heterocyclic carbenes (NHCs) have emerged as a major direction in ancillary ligand development for stabilization of reactive metal centers in inorganic and organometallic chemistry. In particular wingtip-flexible NHCs have attracted significant attention due to their unique ability to provide sterically-demanding environment for transition metals at various oxidation states. Herein, we report a new class of sterically-hindered, wingtip-flexible NHC ligands that feature N,C-chelating oxazole donors. These ligands are readily accessible through a modular arylation of oxazole derivatives. We report the synthesis, full structural and electronic characterization. The evaluation of steric, electron-donating and π-accepting properties and coordination chemistry to Ag(I), Pd(II) and Rh(I) is described. Preliminary catalytic studies in Ag, Pd and Rh-catalyzed coupling and hydrosilylation reactions are presented. The study establishes a fluxional behavior of freely-rotatable oxazole unit, wherein the oxazolyl ring adjusts to the steric and electronic environment of the metal center. Considering the tremendous impact of sterically-hindered NHCs and the potential to stabilize reactive metals by N-chelation, we expect that this class of NHC ligands will be of broad interest in inorganic and organometallic chemistry.

Introduction

Since the seminal studies by Arduengo, N-heterocyclic carbenes (NHCs) have emerged as a powerful class of ligands in various fields of chemistry.[1,2] In particular, in the last two decades, NHCs have played a major role in stabilizing reactive metal centers in inorganic and organometallic chemistry, where the variable steric bulk and strong σ-donation rendered them ligands of choice to provide unique spacial environment around elements.[3–5] Furthermore, these bulky, wingtip-flexible NHC ligands have been deployed in a broad range of catalytic transformations, where their inherent steric and electronic properties enable precise control of the reaction selectivity in many transformations.[6] Other recent applications of NHC ligands involve their use in functional materials, polymers, metal–organic frameworks, and nanoparticles, among other applications.[7,8]

The multifaceted applications spanning diverse areas of chemistry have spurred extensive research efforts towards the synthesis of new classes of N-heterocyclic carbenes. In this respect, studies by Nolan, Glorius, Bertrand, Marko and others[9–13] have led to the successful development of various types of N-heterocyclic carbenes that are now routinely utilized in organometallic chemistry. Among various classes of NHC ligands, the most prominent are sterically-hindered symmetrical ligands based on imidazol-2-ylidene architecture that provide kinetic stabilization of metal centers.[1–5] In this context, N-heterocyclic carbene ligands bearing donor substituents that stabilize metals by chelation are underdeveloped.[14]

As part of our studies on the development of new N-heterocyclic carbenes,[15] herein, we report a new class of sterically-hindered, wingtip-flexible NHC ligands that feature N,C-chelating oxazole donors. We report the synthesis, full structural and electronic characterization. The evaluation of steric, electron-donating and π-accepting properties and coordination chemistry to Ag(I), Pd(II) and Rh(I) is described. We demonstrate a fluxional behavior of freely-rotatable oxazole unit, wherein the oxazolyl ring adjusts to the steric and electronic environment of the metal center. In the context of NHC ligand design, these ligands represent a wide avenue towards expanding the rich field of applications of symmetrical IPr* class of ligands to unsymmetrical, sterically-hindered and chelating IPr*^{Oxa} NHCs. Considering the tremendous impact of sterically-hindered NHCs[9–13] and the potential to stabilize reactive metals by N-chelation,[16,2h] we expect that this new class of NHC ligands will be of broad interest in inorganic and organometallic chemistry.

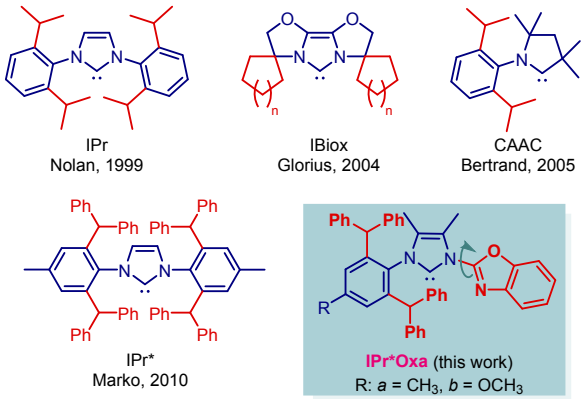

Fig. 1. State-of-the-art of sterically-demanding N-heterocyclic carbenes in inorganic and organometallic chemistry.

[a] Department of Chemistry, Opole University, 48 Oleska Street, Opole 45-052, Poland. E-mail: ebisz@uni.opole.pl
[b] Department of Chemistry, University of Science and Technology, Norwida 4/6, Wroclaw 50-373, Poland
[c] Department of Chemistry, Wroclaw University, F. Joliot-Curie 14, Wroclaw 50-383, Poland
[d] Department of Chemistry, Rutgers University, 73 Warren Street, Newark, NJ 07102, United States. E-mail: michal.szostak@rutgers.edu.
Electronic Supplementary Information (ESI) available: Experimental details and computational data. See DOI: 10.1039/x0xx00000x

Results and Discussion

The synthesis of IPr*^{Oxa} and its MeO analogue featuring $CHPh_2$ wingtips was selected as our starting point (Schemes 1-2, **3a–3b**). This synthesis has been selected on the basis that IPr* and IPr*^{MeO} bearing 2,6-bis(diphenylmethyl)-4-methylphenyl and 2,6-bis(diphenylmethyl)-4-methoxyphenyl wingtips are the two most useful sterically-hindered, wingtip-flexible symmetrical imidazol-2-ylidenes in organometallic chemistry.[12] It is worth noting that IPr*^{MeO} is more nucleophilic than its IPr* counterpart (TEP, Tolman electronic parameter, ν_{CO} IPr*^{MeO} = 2051.1 cm^{-1}; ν_{CO} IPr* = 2052.7 cm^{-1}).[17] Furthermore, the use of 2,6-bis(diphenylmethyl)-4-methoxyphenyl substitution offers synthetic advantages in isolation and crystallization of intermediates and complexes in select cases.[17] The developed synthesis follows a two-step modular approach involving (1) condensation between the corresponding aniline and diacetyl, (2) arylation with 2-halo-benzoxazole (Schemes 1–2). 4,5-Dimethyl substitution of the imidazole ring is preferred due to higher stability of NHC salts and NHC–metal complexes.[18] The developed sequence permits for the preparation of imidazolium precursors **3a–3b** on a gram scale, avoiding chromatographic purification during the synthesis. The imidazolium salts **3a–3b** were obtained as bench-stable, crystalline solids (**3a**, mp = 252-254 °C; **3b**: mp = 197-199 °C). The approach is highly modular enabling the synthesis of analogues by condensation/S_NAr arylation sequence.

Scheme 1 Synthesis of 1-Arylimidazoles **2a–2b**

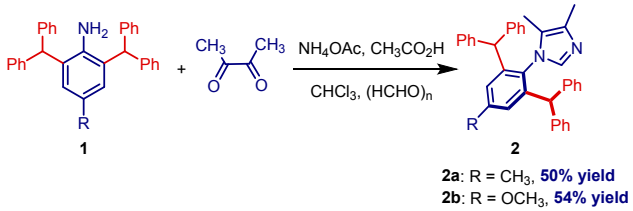

Scheme 2 Synthesis of Imidazolium Salts **3a–3b**

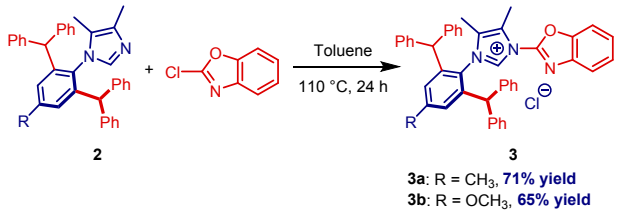

With the access to imidazolium precursors secured, we next evaluated coordination chemistry of these wingtip-flexible, chelating oxazole-donor N-heterocyclic carbene ligands (Schemes 3–6). As shown in Scheme 3, the linear silver complexes [Ag(IPr*^{Oxa})Cl] (**4a**) and [Ag(IPr*^{MeOOxa})Cl] (**4b**) were prepared using method by Gimeno with $AgNO_3$ in the presence of K_2CO_3 at room temperature.[19] The complexes **4a–4b** were found to be stable to air and moisture. The complexes were characterized by X-ray crystallography (Figure 2).

Complexes **4a–4b** are monomeric. Complex **4a** crystallized with three molecules in the unit cell. The coordination around silver is linear ([Ag(IPr*^{Oxa})Cl], C–Ag–Cl, 175.5(15)°, C–Ag, 2.079(5) Å; C–Ag–Cl, 172.4(18)°, C–Ag, 2.074(6) Å; C–Ag–Cl, 178.74(16)°, C–Ag, 2.087(5) Å; [Ag(IPr*^{MeOxa})Cl], C–Ag–Cl, 173.09(18)°; C–Ag, 2.075(6) Å). Interestingly, the oxazolyl ring is close to coplanar with the imidazolyl ring with the oxygen atom oriented towards the metal in [Ag(IPr*^{Oxa})Cl] ([Ag(IPr*^{Oxa})Cl], O–Ag, 3.055(4) Å; O–Ag, 2.875(4) Å;

Scheme 3 Synthesis of Ag(I)–NHC Complexes **4a–4b**

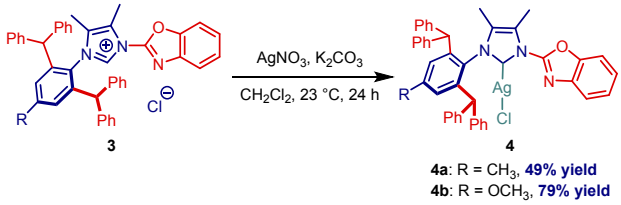

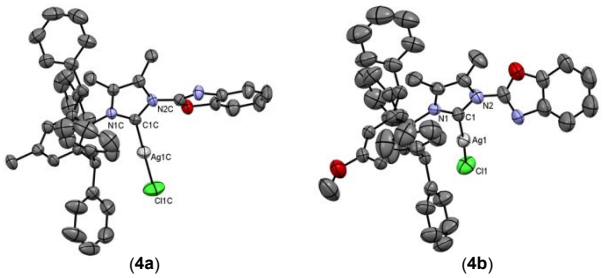

Fig. 2. X-ray crystal structures of complexes **4a–4b**. CCDC 2180038, **4a**; CCDC 2180039, **4b**. See SI for selected bond lengths and angles.

Scheme 4 Synthesis of Pd(II)–NHC Complexes **5a–5b**

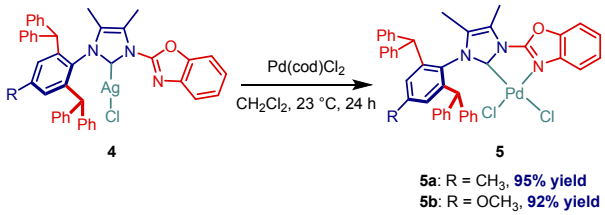

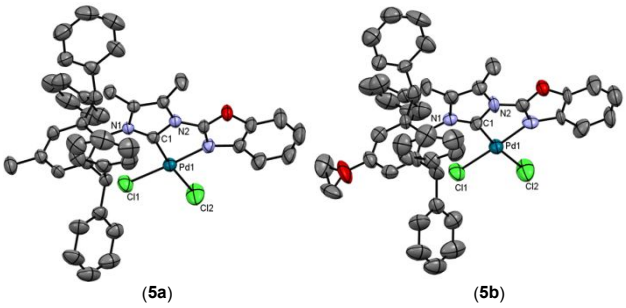

Fig. 3. X-ray crystal structures of complexes **5a–5b**. CCDC 2180040, **5a**; CCDC 2180041, **5b**. See SI for selected bond lengths and angles.

O–Ag, 3.114(3) Å), while the oxazolyl ring is tilted with respect to the imidazolyl ring in [Ag(IPr*^{MeOOxa})Cl] with the nitrogen atom pointing towards the metal ([Ag(IPr*^{MeOOxa})Cl], N–Ag, 3.264(6) Å). The dihedral angle in [Ag(IPr*^{Oxa})Cl] of $C_{(carbene)}$–N–C–O is 23.0(7)°, 18.1(8)°, 40.2(7)° for the three molecules in the until cell, and the angle between the planes of the oxazolyl and imidazolyl ring is 23.8(2)°, 17.5(2)°, 37.8(2)°. The dihedral angle in [Ag(IPr*^{MeOOxa})Cl] of $C_{(carbene)}$–N–C–N is 44.7(11)° and the angle between the planes of the oxazolyl and imidazolyl ring is 44.3(1)°. The geometry of complexes **4a–4b** was analyzed using the method by Cavallo[20] to determine catalytic pockets (Chart 1A–1B). The % buried volume (%V_{bur}) of [Ag(NHC)Cl] complexes **4a–4b** is 43.3%, 42.7%, 39.6% (**4a**, 3 molecules in the unit cell) and 40.7% (**4b**). These values can be compared with [Ag(IPr*)Cl] of 53.5%[12] and [Ag(IPr)Cl] of 43.8%.[21] It should be noted that the classical imidazol-2-ylidenes feature a more symmetrical quadrant distribution, while IPr*^{Oxa} ligands have a clear steric differentiation between SW/NW vs. NE/SE quadrants (Chart 1).

Scheme 5 Synthesis of Se–NHC Complex **6a**

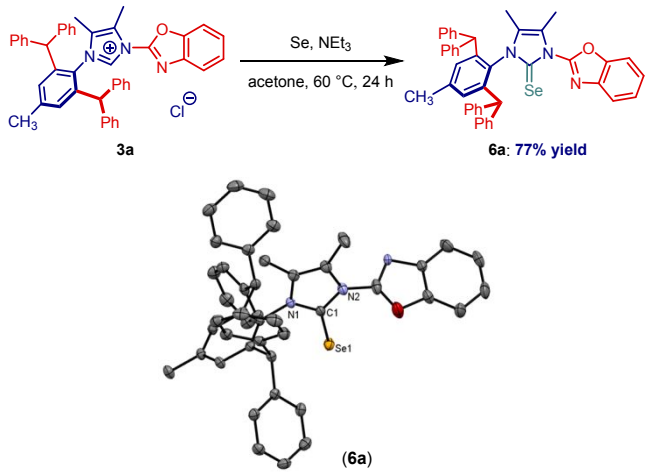

Fig. 4. X-ray crystal structure of complex **6a**. CCDC 2180042, **6a**. See SI for selected bond lengths and angles.

Scheme 6 Synthesis of [RhCl(NHC)(CO)] Complex **7a**

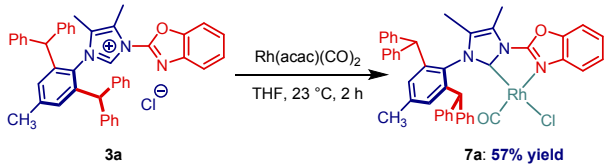

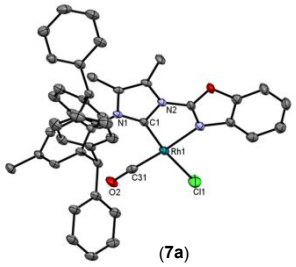

Fig. 5. X-ray crystal structure of complex **7a**. CCDC 2180043, **7a**. See SI for selected bond lengths and angles.

Next, we synthesized chelating [Pd(IPr*^{Oxa})Cl$_2$] (**5a**) and [Pd(IPr*^{MeOxa})Cl$_2$] (**5b**) complexes by transmetallation of **4a–4b** with [Pd(cod)Cl$_2$] (Scheme 4). The structures of complexes **5a–5b** were determined by x-ray crystallography (Figure 3). The geometry around palladium is square planar with the oxazolyl and imidazolyl rings coplanar ([Pd(IPr*^{Oxa})Cl$_2$], C$_{(carbene)}$–N–C–N, 0.0°; [Pd(IPr*^{MeOOxa})Cl$_2$], C$_{(carbene)}$–N–C–N, 0.0°). In [Pd(IPr*^{Oxa})Cl$_2$], the bond lengths of C$_{(carbene)}$–Pd, 1.993(3) Å; N$_{(oxazolyl)}$–Pd, 2.047(3) Å are in the range for N,C chelating Pd(II)–NHC complexes.[14f,g] There is a strong trans influence of the NHC ligand, C$_{(carbene)}$Pd–Cl, 2.3256(12) Å; N$_{(oxazolyl)}$Pd–Cl, 2.2675(11) Å. Similar bond lengths are observed in [Pd(IPr*^{MeOOxa})Cl$_2$] of C$_{(carbene)}$–Pd, 1.985(10) Å; N$_{(oxazolyl)}$–Pd, 2.067(8) Å; C$_{(carbene)}$Pd–Cl, 2.311(3) Å; N$_{(oxazolyl)}$Pd–Cl, 2.267(3) Å.

The geometry of complexes **5a–5b** was further analyzed using the method by Cavallo to determine the % buried volume (Chart 1C–1D). The (%V_{bur}) of [Pd(NHC)Cl$_2$] complexes **5a–5b** is 40.8% (**5a**) and 40.6% (**5b**). These values can be compared with the linear Ag(I)–NHC complexes **4a–4b** (Chart 1A–1B). It should be noted that the oxazolyl fragment in **4a–4b** has rotated to be coplanar with the Pd atom, which is reflected by the quadrant distribution in the topographical steric maps in IPr*^{Oxa} ligands.

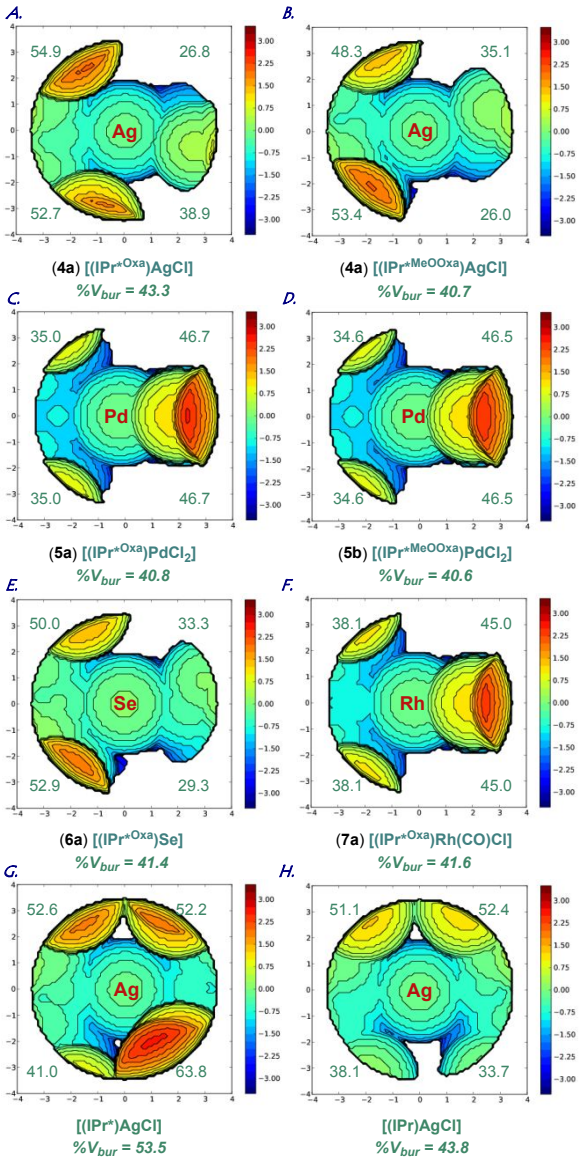

Chart 1. Topographical steric maps of (A) [(IPr*^{Oxa})AgCl] (**4a**), (B) [(IPr*^{MeOOxa})AgCl] (**4b**), (C) [(IPr*^{Oxa})PdCl$_2$] (**5a**), (D) [(IPr*^{MeOOxa})PdCl$_2$] (**5b**), (E) [(IPr*^{Oxa})Se] (**6a**), (F) [(IPr*^{Oxa})Rh(CO)Cl] (**7a**) showing %V_{bur} per quadrant. (G) [(IPr*)AgCl] and (H) [(IPr)AgCl] are shown for comparison.

To evaluate electronic properties of this class of N,C-chelating ligands, we prepared the selenourea adduct **6a** (Scheme 5). Seleno adducts permit to evaluate π-backbonding from the ^{77}Se NMR spectra.[22] The standard method developed by Nolan et al was used for ^{77}Se measurements.[22] IPr*^{Oxa} **3a** was selected as a representative NHC for Se and Rh (*vide infra*) measurements. In our experience, ^{77}Se measurements are strongly affected by the type of heterocyclic system, however, tilt of the wingtip should also be taken into consideration in select cases.[22] To our knowledge, this is the first example of ^{77}Se measurements for NHCs with a wingtip-flexible O atom.[5,22] The δSe value of 119.4 ppm for [Se(IPr*^{Oxa})] ($CDCl_3$) can be compared with IPr (δSe = 90 ppm) and IPr* (δSe = 106 ppm), suggesting slightly higher π-accepting properties, expected from the oxazolyl substitution. The structure of **6a** was determined by x-ray crystallography (Figure 4). The C–Se bond length is 1.831(4) Å. The oxazolyl ring is significantly tilted with respect to the imidazolyl ring (C$_{(carbene)}$–N–C–O, 70.1(6)°) with the oxygen atom point towards selenium, Se–O, 3.549(3) Å. The (%V_{bur}) of [Se(IPr*^{Oxa})] complex is

41.4% (**6a**) (SW, 52.9%; NW, 50.0%; NE, 33.3%; SE, 29.3%) (Chart 1E). Compared with the linear [Ag(IPr*^{Oxa})Cl] complex **4a**, the oxazolyl ring further rotates away from the metal center in [Se(IPr*^{Oxa})], highlighting flexibility of the N–oxazolyl wingtip.

We also synthesized the chelating [Rh(IPr*^{Oxa})(CO)Cl] complex as a representative cationic Rh(I) complex to further evaluate the electronic properties of this class of ligands.

Scheme 7 Catalytic Activity of [IPr*^{Oxa}–M] Complexes[a]

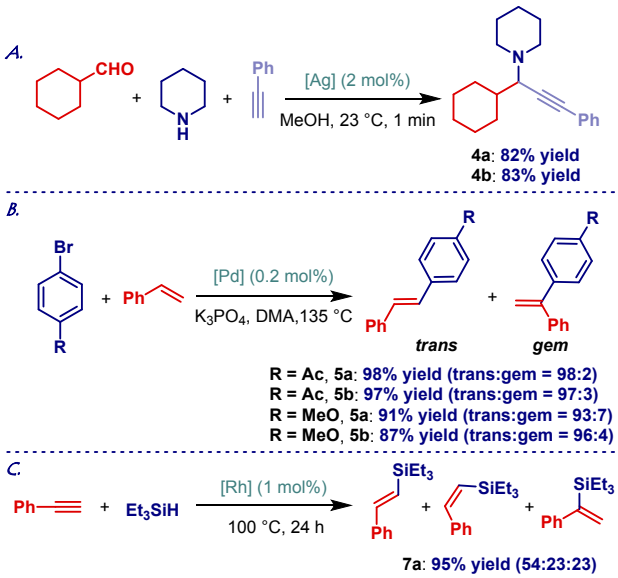

[Rh(IPr*^{Oxa})(CO)Cl] (**7a**) was prepared by the direct reaction of the imidazolium precursor **3a** and [Rh(acac)(CO)$_2$] (Scheme 6). The complex is characterized by the CO stretching of 1986 cm^{-1}. This can be compared with related cationic N,C-chelating Rh(I)–NHC complexes [Rh(NHC)(CO)$_2$](OTf) of 2017 and 2076 cm^{-1}.[23] The structure of **7a** was determined by x-ray crystallography (Figure 5). The geometry around rhodium is square planar with the oxazolyl and imidazolyl rings coplanar ($C_{(carbene)}$–N–C–N, 0.0°). The bond lengths of $C_{(carbene)}$–Rh, 1.976(4) Å; $N_{(oxazolyl)}$–Rh, 2.131(3) Å are in the range for N,C chelating Rh(I)–NHC complexes.[14f,g,23] The Cl ligand is positioned trans to the carbene (Rh–Cl, 2.3705(11) Å), while the CO ligand is positioned trans to the oxazolyl ring (Rh–CO, 1.796(4) Å). The (%V_{bur}) of [Rh(IPr*^{Oxa})(CO)Cl] complex is 41.6% (**7a**) (SW, 38.1%; NW, 38.1%; NE, 45.0%; SE, 45.0%) (Chart 1F), which can be compared with the chelating Pd(II) complex **5a** of 40.8% (Chart 1C).

We briefly evaluated the catalytic activity of the sterically-hindered N,C-chelating oxazolyl-donor ligands in Ag(I), Pd(0) and Rh(I) catalyzed coupling and hydrosilylation reactions (Scheme 7). As shown, [Ag(IPr*^{Oxa})Cl] (**4a**), [Ag(IPr*^{MeOOxa})Cl] (**4b**), [Pd(IPr*^{Oxa})Cl$_2$] (**5a**), [Pd(IPr*^{MeOxa})Cl$_2$] (**5b**) and [Rh(IPr*^{Oxa})(CO)Cl] (**7a**) gave promising reactivity in A3-coupling, Heck cross-coupling and alkyne hydrosilation. The results indicate high degree of generality of this class of ligands in C–N, C–C and C–Si bond forming reactions. The results should be benchmarked against prior systems. Thus, complexes [Ag(IPr*^{Oxa})Cl] (**4a**) and [Ag(IPr*^{MeOOxa})Cl] (**4b**) are more reactive than the classical [Ag(IPr)Cl],[25a] while [Pd(IPr*^{Oxa})Cl$_2$] (**5a**) and [Pd(IPr*^{MeOxa})Cl$_2$] (**5b**) show similar reactivity to Pd(II)–NHC complexes with oxazolinyl wingtip,[14f] however, higher trans selectivity of (**5b**) should be noted. Finally, [Rh(IPr*^{Oxa})(CO)Cl] (**7a**) should be compared with Rh(I)–NHCs containing hemilabile N-donors, which typically give higher *E*-selectivity.[26]

To gain insight into the electronic structure of the IPr*^{Oct} class of ligands, we determined HOMO and LUMO energy levels at the B3LYP 6-311++g(d,p) level (Figure 6 and SI). It is now well established that computed HOMO and LUMO provide the most accurate determination of nucleophilicity and electrophilicity of N-heterocyclic carbene ligands. The σ-donor orbital of IPr*^{Oxa} (HOMO-1 due to required symmetry, -6.26 eV) is in the same range as IPr* (-6.12 eV), and can be compared with the classical IPr (-6.01 ev). The HOMO-1 of IPr*^{MeOOxa} is marginally higher (-6.22 eV), as expected from the MeO substitution. The π-accepting orbital (LUMO+8 due to required symmetry) of IPr*^{Oxa} (-0.33 eV) and IPr*^{MeOOxa} (-0.32 eV) can be compared with IPr* (-0.90 eV) and IPr (-0.48 eV). The LUMO orbital of IPr*^{Oxa} (-1.18 eV) and IPr*^{MeOOxa} (-1.17 eV) is located on the benzoxazole ring as expected. Overall, these results confirm IPr*^{Oxa} and IPr*^{MeOOxa} as strongly σ-nucleophilic, sterically-unsymmetrical N-heterocyclic carbene ligands with electronics affected by the coordinating benzoxazole ring.

Furthermore, rotational studies were performed to gain insight into the fluxional character of the N–oxazolyl wingtip in this IPr*^{Oxa} class of ligands (Figure 7). Detailed rotational profile of the parent carbene IPr*^{Oxa} was obtained by a systematic rotation along the $C_{(Me)}$–N–$C_{(oxa)}$–O dihedral angle. The rotation was performed in both directions. The rotational profile of IPr*^{Oxa} identified two energy minima at ca. 160° $C_{(Me)}$–N–$C_{(oxa)}$–O angle in a syn eclipsing $C_{(carbene)}$–N–$C_{(oxa)}$–O conformation (ca. 22.2°) (0 kcal/mol) and at ca. 50° in a gauche $C_{(carbene)}$–N–$C_{(oxa)}$–N conformation (ca. 49.1°) (2.3 kcal/mol). The energy maxima are located at ca. 0° $C_{(Me)}$–N–$C_{(oxa)}$–O dihedral angle (3.5 kcal/mol) in a syn eclipsing $C_{(carbene)}$–N–$C_{(oxa)}$–N conformation (ca. 0.0°) and at ca. 80° $C_{(carbene)}$–N–$C_{(oxa)}$–O dihedral angle (2.6 kcal/mol) in a perpendicular $C_{(carbene)}$–N–$C_{(oxa)}$–N conformation (ca. 80.5°). The rotational profile of IPr*^{Oxa} provides further evidence for the flexible rotation of the N-oxazole wingtip.

As shown by the complexation with Ag(I), Pd(II) and Rh(I), the ligand geometry hinges upon the interaction with the metal in a N,C-chelating template. The combination of the large sterically-demanding IPr*-type substitution with the flexibility of the N-benzoxazole wingtip provides a sterically-encumbered chelating environment around the metal centers (Charts 1A–1G).

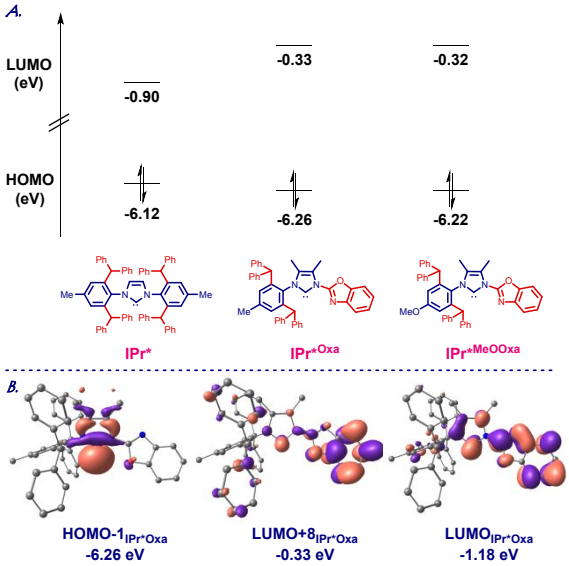

Fig. 6. (A) HOMO and LUMO energy levels (eV). (B) HOMO-1, LUMO+8 and LUMO (eV) of IPr*^{Oxa} calculated at B3LYP 6-311++g(d,p). See SI.

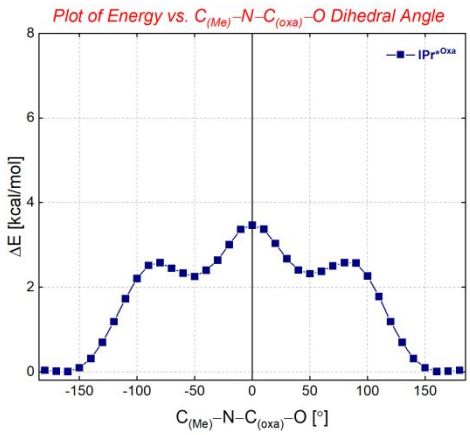

Fig. 7. Rotational profile of IPr*^{Oxa} (ΔE, kcal/mol, vs. C(Me)–N–C(oxa)–O [°]).

Conclusions

In conclusion, we have reported a new class of sterically-hindered, wingtip-flexible NHC ligands that feature N,C-chelating oxazole donors. These ligands combine the properties of symmetrical and broadly utilized IPr* class of ligands with N,C-chelating donors. The ligands are readily accessible through a modular arylation of oxazole derivatives. The coordination chemistry was demonstrated through the synthesis and full structural characterization of Ag(I), Pd(II) and Rh(I) complexes. The study established a fluxional behavior of freely-rotatable oxazole ring, adjusting to the steric and electronic environment of the metal center. In light of the tremendous impact of sterically-hindered NHCs and the potential to stabilize reactive metals by N-chelation, this new class of NHC ligands opens new avenues in inorganic and organometallic chemistry.

Experimental

General methods. All experiments involving metal complexes were performed using standard Schlenk techniques under nitrogen or argon unless stated otherwise. All solvents were purchased at the highest commercial grade and used as received or after purification by distillation from sodium/benzophenone under nitrogen. All solvents were deoxygenated prior to use. All other chemicals were purchased at the highest commercial grade and used as received. Compounds **1a**,[12a] **1b**,[17] and **2a**[18] have been previously reported in the literature. Spectroscopic properties matched literature data. ^{1}H NMR and ^{13}C NMR spectra were recorded on Bruker spectrometers at 400 (^{1}H NMR) and 100 MHz (^{13}C NMR). Infrared spectra were recorded on a Nicolet Nexus 2002 FTIR spectrometer. High-resolution mass spectra (HRMS) and elemental analyses were measured on a 7T Bruker Daltonics FT-MS and Vario EL II (CHNS) instrument respectively.

General Procedure for the Synthesis of Anilines. Anilines were synthesized according to literature procedures.[12a,17]

2,6-Dibenzhydryl-4-methylaniline (1a).[below12a] The product was obtained in 52% yield (24.00 g, 54.6 mmol) as a white solid. ^{1}H NMR (400 MHz, $CDCl_3$) δ 7.27 (t, *J* = 7.2 Hz, 10H, H_{Ar}), 7.23 – 7.19 (m, 2H, H_{Ar}), 7.09 (d, *J* = 7.0 Hz, 8H, H_{Ar}), 6.38 (s, 2H, H_{Ar}), 5.45 (s, 2H, CH_{Ph2}), 3.27 (s, 2H, NH_2), 2.01 (s, 3H, CH_3). ^{13}C NMR (100 MHz, $CDCl_3$) δ 142.90 (C_{Ar}), 139.78 (C_{Ar}), 129.69 (CH_{Ar}), 129.38 (C_{Ar}), 129.18 (CH_{Ar}), 128.63 (CH_{Ar}), 126.74 (CH_{Ar}), 52.51(CH_{Ph2}), 21.17 (CH_3).

4-Methoxy-2,6-bis(diphenylmethyl)aniline (1b).[17] The product was obtained in 93% yield (44.00 g, 96.6 mmol) as a white solid. ^{1}H NMR (400 MHz, $CDCl_3$) δ 7.27 (t, *J* = 8.2 Hz, 8H, H_{Ar}), 7.21 (t, *J* = 8.2 Hz, 4H, H_{Ar}), 7.09 (d, *J* = 7.2 Hz, 8H, H_{Ar}), 6.19 (s, 2H, H_{Ar}), 5.47 (s, 2H, CH_{Ph2}), 3.41 (s, 3H, OCH_3), 3.13 (s, 2H, NH_2). ^{13}C NMR (101 MHz, $CDCl_3$) δ 151.93 (C_{Ar}), 142.63 (C_{Ar}), 136.03 (CH_{Ar}), 130.95 (C_{Ar}), 129.65 (CH_{Ar}), 128.68 (CH_{Ar}), 126.86 (CH_{Ar}), 114.49 (CH_{Ar}), 55.26 (OCH_3), 52.61 (CH_{Ph2}).

General Procedure for the Synthesis of 1-Arylimidazoles. *N*-Aryl imidazoles were synthesized according to a modified literature procedure.[18] To a aniline derivative (12 mmol) in dry $CHCl_3$ (20 mL), diacetyl (10 mmol), acetic acid (50 mmol), NH_4OAc (12 mmol), paraformaldehyde (10 mmol), and H_2O (0.5 mL) were added and the mixture was refluxed for 48 h. After removal of the solvent, the dark residue was dissolved in Et_2O and basified to pH 14 in an ice bath with aqueous 40% KOH solution. The resulting mixture was extracted with Et_2O, and the combined organic layers were washed with H_2O and dried over Na_2SO_4. Concentration and purification through silica gel column chromatography gave the desired product.

1-(2,6-Dibenzhydryl-4-methylphenyl)-4,5-dimethyl-1*H*-imidazole (2a).[18] The product was obtained in 50% yield (2.00 g, 3.85 mmol) as a pale brown solid. Purification by flash chromatography (hexane/AcOEt = 2/1). ^{1}H NMR (400 MHz, $CDCl_3$) δ 7.24 – 7.16 (m, 12H, H_{Ar}), 6.95 (d, *J* = 7.1 Hz, 4H, H_{Ar}), 6.89 (d, *J* = 7.1 Hz, 4H, H_{Ar}), 6.87 (s, 2H, H_{Ar}), 6.62 (s, 1H, H_{Ar}), 5.00 (s, 2H, CH_{Ph2}), 2.25 (s, 3H, $CH_{3\ imid}$), 2.16 (s, 3H, $CH_{3\ imid}$), 1.0 (s, 3H, CH_3). ^{13}C NMR (101 MHz, $CDCl_3$) δ 142.88 (C_{Ar}), 142.86 (C_{Ar}), 142.44 (C_{Ar}), 138.96 (C_{Ar}), 135.63 (CH_{Ar}), 133.76 (C_{Ar}), 132.31 (C_{Ar}), 129.69 (CH_{Ar}), 129.63 (CH_{Ar}), 129.26 (CH_{Ar}), 128.55 (CH_{Ar}), 128.39 (CH_{Ar}), 126.69 (CH_{Ar}), 126.67 (CH), 123.54 (C_{Ar}), 51.53 (CH_{Ph2}), 21.95 (CH_3), 12.96 ($CH_{3\ imid}$), 7.90 ($CH_{3\ imid}$).

1-(2,6-Dibenzhydryl-4-methoxyphenyl)-4,5-dimethyl-1*H*-imidazole (2b). The product was obtained in 54% yield (2.17g, 4.06 mmol) as a pale yellow solid. Mp = 87-89 °C. Purification by flash chromatography (hexane/AcOEt = 2/1). ^{1}H NMR (400 MHz, $CDCl_3$) δ 7.24 – 7.16 (m, 12H, H_{Ar}), 6.96 (d, *J* = 6.8 Hz, 4H, H_{Ar}), 6.90 (d, *J* = 6.9 Hz, 4H, H_{Ar}), 6.57 (s, 3H, H_{Ar}), 5.00 (s, 2H, CH_{Ph2}), 3.61 (s, 3H, CH_3), 2.15 (s, 3H, $CH_{3\ imid}$), 1.30 (s, 3H, $CH_{3\ imid}$). ^{13}C NMR (100 MHz, $CDCl_3$) δ 159.39 (C_{Ar}), 144.61 (C_{Ar}), 142.63 (C_{Ar}), 142.21 (C_{Ar}), 135.95 (CH_{Ar}), 133.85 (C_{Ar}), 129.58 (CH_{Ar}), 129.18 (CH_{Ar}), 128.57 (CH_{Ar}), 128.41 (CH_{Ar}), 127.83 (CH_{Ar}), 126.76 (CH_{Ar}), 123.55 (C_{Ar}), 114.44 (CH_{Ar}), 55.38 (CH_3), 51.75 (CH_{Ph2}), 13.09 ($CH_{3\ imid}$), 7.88 ($CH_{3\ imid}$). HRMS (ESI/Q-TOF) m/z: $[M+H]^+$ calcd for $C_{38}H_{35}N_2O$ 535.2749 found 535.2702.

General Procedure for the Synthesis of Imidazolium Salts. Imidazolium salts were synthesized according to a literature procedure.[14g] 1-Arylimidazole (2a or 2b) was added to a solution of 2-chlorobenzoxazole in toluene, and the mixture was heated at reflux overnight. During the course of the reaction, a white precipitate formed and the product was isolated by filtration. The solid was washed twice with Et_2O and dried in vacuo, giving the desired imidazolium salt.

1-(Benzo[*d*]oxazol-2-yl)-3-(2,6-dibenzhydryl-4-methylphenyl)-4,5-dimethyl-1*H*-imidazol-3-ium Chloride (3a). The product was obtained in 71% yield (2.00 g, 3.86 mmol) as a white solid. Mp = 252-254 °C. ^{1}H NMR (400 MHz, $CDCl_3$) δ 10.51 (s, 1H, NCHN), 7.78-7.72 (m, 2H, CH_{oxa}), 7.49 – 7.43 (m, 2H, CH_{oxa}), 7.25 – 7.17 (m, 14H, H_{Ar}), 7.11 (d, J = 5.4 Hz, 2H, H_{Ar}), 7.02 (d, J = 7.1 Hz, 4H, H_{Ar}), 6.79 (s, 2H, H_{Ar}), 5.35 (s. 2H, CH_{Ph2}), 2.62 (s, 3H, $CH_{3\ imid}$), 2.23 (s, 3H, $CH_{3\ imid}$), 1.28 (s, 3H, CH_3). ^{13}C NMR (101 MHz, $CDCl_3$) δ 149.05 (NCO), 148.66 (C_{oxa}), 142.03 (C_{oxa}), 141.80 (C_{Ar}), 141.31 (C_{Ar}), 140.36 (C_{Ar}), 139.81 (N_2C), 138.85 (CH_{Ar}), 130.71 (C_{Ar}), 130.19 (C_{Ar}), 129.74 (CH_{Ar}), 129.38 (CH_{Ar}), 128.89 (CH_{Ar}), 128.82 (CH_{Ar}), 128.35 (CH_{Ar}), 127.32 (C_{Ar}), 127.04 (CH_{Ar}), 126.61 (CH_{Ar}), 126.08 (CH_{Ar}), 120.73 (CH_{Ar}), 111.91 (CH_{Ar}),

52.07 (CH_{Ph2}), 22.04 (CH_3), 10.98 ($CH_{3\ imid}$), 7.80 ($CH_{3\ imid}$). HRMS (ESI/Q-TOF) m/z: $[M]^+$ calcd for $C_{45}H_{38}N_3O$ 636.3015 found 636.3015.

1-(Benzo[*d*]oxazol-2-yl)-3-(2,6-dibenzhydryl-4-methoxyphenyl)-4,5-dimethyl-1*H*-imidazol-3-ium Chloride (3b). The product was obtained in 65% yield (0.8 g, 1.22 mmol) as a white solid. Mp = 197-199 °C. ^{1}H NMR (400 MHz, $CDCl_3$) δ 10.50 (s, 1H, NCHN), 7.75 (dd, *J* = 13.1, 4.3 Hz, 2H, CH_{oxa}), 7.49 – 7.45 (m, 2H, CH_{oxa}), 7.28 – 7.21 (m, 14H, H_{Ar}), 7.13 – 7.09 (m, 2H, H_{Ar}), 7.04 (d, *J* = 6.5 Hz, 4H, H_{Ar}), 6.48 (s, 2H, H_{Ar}), 5.38 (s, 2H, CH_{Ph2}), 3.56 (s, 3H, CH_3), 2.61 (s, 3H, $CH_{3\ imid}$), 1.30 (s, 3H, $CH_{3\ imid}$). ^{13}C NMR (100 MHz, $CDCl_3$) δ 161.08 (NCO), 149.07 (C_{oxa}), 148.70 (C_{oxa}), 144.13 (C_{Ar}), 141.06 (C_{Ar}), 140.25 (C_{Ar}), 139.84 (N_2C), 139.27 (CH_{Ar}), 130.32 (C_{Ar}), 129.73 (CH_{Ar}), 129.37 (CH_{Ar}), 128.96 (CH_{Ar}), 128.86 (CH_{Ar}), 127.41 (CH_{Ar}), 127.16 (C_{Ar}), 127.06 (CH_{Ar}), 126.51 (CH_{Ar}), 126.09 (CH_{Ar}), 123.41 (CH_{Ar}), 120.73, 115.56, 111.94 (CH_{Ar}), 55.36 (CH_3), 52.27 (CH_{Ph2}), 11.01 ($CH_{3\ imid}$), 7.82 ($CH_{3\ imid}$). HRMS (ESI/Q-TOF) m/z (%) $[M]^+$ calcd for $C_{45}H_{38}N_3O_2$ 652.2964; found 652.2953.

General Procedure for the Synthesis of [Ag(NHC)Cl] Complexes. Ag(I)–NHC complexes were synthesized according to a modified literature procedure.[19] A mixture of imidazolium salt (3a or 3b) and $AgNO_3$ in dichloromethane was stirred for 2 min and then K_2CO_3 was added. After 24 h, the mixture was filtered through Celite and the solvent was removed in vacuo until 2 mL (c.a.). The product was precipitated with ether and washed to give a white solid.

[Ag(IPr*^{Oxa})Cl] (4a). The product was obtained in 49% yield (0.13 g, 0.17 mmol) as a white solid. Recrystallization from CH_2Cl_2/Et_2O at RT gave suitable crystals for X-ray diffraction analysis. ^{1}H NMR (400 MHz, $CDCl_3$) δ 7.80 – 7.76 (m, 1H, CH_{oxa}), 7.67 – 7.63 (m, 1H, CH_{oxa}), 7.45 – 7.42 (m, 2H, CH_{oxa}), 7.28 – 7.17 (m, 12H, H_{Ar}), 7.04 (d, *J* = 7.4 Hz, 4H, H_{Ar}), 6.95 (d, *J* = 6.5 Hz, 4H, H_{Ar}), 6.81 (s, 2H, H_{Ar}), 5.24 (s, 2H, CH_{Ph2}), 2.41 (s, 3H, $CH_{3\ imid}$), 2.26 (s, 3H, $CH_{3\ imid}$), 1.07 (s, 3H, CH_3). ^{13}C NMR (100 MHz, $CDCl_3$) δ 186.38 (N_2C), 186.21 (N_2C), 183.84 (N_2C), 183.66 (N_2C), 152.72 (NCO), 149.25 (C_{oxa}), 142.19 (C_{Ar}), 141.49 (C_{Ar}), 140.97 (C_{Ar}), 140.27 (C_{Ar}), 140.19 (C_{oxa}), 133.42 (C_{Ar}), 130.34 (CH_{Ar}), 129.83 (CH_{Ar}), 129.39 (CH_{Ar}), 129.08 (CH_{Ar}), 128.64 (C_{Ar}), 127.13 (CH_{Ar}), 127.11 (CH_{Ar}), 126.23 (CH_{Ar}), 126.00 (CH_{Ar}), 125.94 (C_{Ar}), 125.69 (CH_{Ar}), 120.47 (CH_{Ar}), 111.42 (CH_{Ar}), 52.03 (CH_{Ph2}), 22.00 (CH_3), 10.87 ($CH_{3\ imid}$), 8.12 ($CH_{3\ imid}$). Anal. calcd for $C_{45}H_{37}AgClN_3O$ (779.13): C, 69.37; H, 4.79; N, 5.39. Found: C, 69.79; H, 4.64; N, 5.44.

[Ag(IPr*^{MeOOxa})Cl] (4b). The product was obtained in 79% yield (0.19 g, 0.24 mmol) as a white solid. Recrystallization from CH_2Cl_2/Et_2O at RT gave suitable crystals for X-ray diffraction analysis. ^{1}H NMR (400 MHz, $CDCl_3$) δ 7.80 – 7.76 (m, 1H, CH_{oxa}), 7.67 – 7.64 (m, 1H, CH_{oxa}), 7.45 – 7.42 (m, 2H, CH_{oxa}), 7.29 – 7.18 (m, 12H, H_{Ar}), 7.06 (d, *J* = 7.4 Hz, 4H, H_{Ar}), 6.98 – 6.95 (m, 4H, H_{Ar}), 6.51 (s, 2H, H_{Ar}), 5.25 (s, 2H, CH_{Ph2}), 3.60 (s, 3H), 2.40 (s, 3H, ($CH_{3\ imid}$), 1.09 (s, 3H, ($CH_{3\ imid}$). ^{13}C NMR (101 MHz, $CDCl_3$) δ 186.83 (N_2C), 186.65 (N_2C), 184.29 (N_2C), 184.11 (N_2C), 160.12 (C_{Ar}), 152.72 (NCO), 149.25 (C_{oxa}), 144.09 (C_{Ar}), 141.20 (C_{Ar}), 140.75 (C_{Ar}), 140.20 (C_{oxa}), 129.78 (C_{Ar}), 129.36 (CH_{Ar}), 129.14 (CH_{Ar}), 128.68 (CH_{Ar}), 127.24 (CH_{Ar}), 127.20 (CH_{Ar}), 126.23 (CH_{Ar}), 125.92 (CH_{Ar}), 125.87 (CH_{Ar}), 125.69 (CH_{Ar}), 120.47 (CH_{Ar}), 115.14 (CH_{Ar}), 111.42 (CH_{Ar}), 55.37 (CH_{Ph2}), 52.29 (CH_3), 10.89 ($CH_{3\ imid}$), 8.13 ($CH_{3\ imid}$). Anal. calcd for $C_{45}H_{37}AgClN_3O_2$ (795.13): C, 67.98; H, 4.69; N, 5.28. Found: C, 68.12; H, 4.75; N, 5.20.

General Procedure for the Synthesis of [Pd(NHC)Cl_2] Complexes. Palladium complexes were synthesized according to a modified literature procedure.[14f] [$PdCl_2$(1,5-COD)] was added to a solution of Ag(I)–NHC complex (4a or 4b) in CH_2Cl_2 with exclusion of light. The mixture became cloudy immediately. After one night at room temperature, the solution was filtered through Celite. The solvent was removed in vacuo.

[Pd(IPr*^{Oxa})Cl_2] (5a). The product was obtained in 95% yield (0.20 g, 0.25 mmol) as a yellow solid. Recrystallization from CH_2Cl_2/Hex at RT gave suitable crystals for X-ray diffraction analysis. ^{1}H NMR (400 MHz, CD_2Cl_2) δ 8.99 (d, *J* = 5.4 Hz, 1H, CH_{oxa}), 7.82 (s, 1H, CH_{oxa}), 7.66 (t, *J* = 8.2 Hz, 2H, CH_{oxa}), 7.43 (d, *J* = 7.1 Hz, 4H, H_{Ar}), 7.39 – 7.35 (m, 4H, H_{Ar}), 7.30 (d, *J* = 5.2 Hz, 8H, H_{Ar}), 7.11 – 7.07 (m, 4H, H_{Ar}), 6.94 (s, 2H, H_{Ar}), 5.57 (s, 2H, CH_{Ph2}), 2.37 (s, 3H, $CH_{3\ imid}$), 2.29 (s, 3H, $CH_{3\ imid}$), 0.00 (s, 3H, CH_3). ^{13}C NMR (101 MHz, CD_2Cl_2) δ 157.58 (C_{Ar}), 154.81 (NCO), 149.34 (C_{oxa}), 142.34 (C_{Ar}), 141.45 (C_{Ar}), 140.22 (C_{Ar}), 139.84 (C_{oxa}), 136.40 (C_{Ar}), 133.53 (C_{Ar}), 132.23 (C_{Ar}), 129.96 (CH_{Ar}), 129.82 (CH_{Ar}), 129.75 (CH_{Ar}), 128.44 (CH_{Ar}), 128.17 (CH_{Ar}), 127.69 (CH_{Ar}), 127.01 (CH_{Ar}), 126.54 (CH_{Ar}), 122.15 (CH_{Ar}), 120.70 (CH_{Ar}), 111.39 (CH_{Ar}), 51.90 (CH_{Ph2}), 21.60 (CH_3), 8.53 ($CH_{3\ imid}$), 6.47 ($CH_{3\ imid}$). Anal. calcd for $C_{45}H_{37}Cl_2N_3OPd$ (813.13): C, 66.47; H, 4.59; N, 5.17. Found: C, 66.34; H, 4.41; N, 5.02.

[Pd(IPr*^{MeOOxa})Cl_2] (5b). The product was obtained in 92% yield (0.19 g, 0.23 mmol) as a yellow solid. Recrystallization from CH_2Cl_2/Hex at RT gave suitable crystals for X-ray diffraction analysis. ^{1}H NMR (400 MHz, $CDCl_3$): δ 8.89 (d, *J* = 8.1 Hz, 1H, CH_{oxa}), 7.58 (d, *J* = 7.9 Hz, 1H, CH_{oxa}), 7.48 – 7.42 (m, 2H, CH_{oxa}), 7.29 (d, *J* = 7.6 Hz, 4H, H_{Ar}), 7.18 – 7.09 (m, 12H, H_{Ar}), 6.94 – 6.92 (m, 4H, H_{Ar}), 6.42 (s, 2H, H_{Ar}), 5.42 (s, 2H, CH_{Ph2}), 3.51 (s, 3H, $CH_{3\ imid}$), 2.14 (s, 3H, $CH_{3\ imid}$), -0.08 (s, 3H, CH_3). ^{13}C NMR (101 MHz, $CDCl_3$): δ 159.91 (N=CO), 157.21 (C_{Ar}), 155.82 (NCO), 149.15 (C_{oxa}), 143.22 (C_{Ar}), 141.63 (C_{Ar}), 140.09 (C_{oxa}), 136.31 (C_{Ar}), 133.56 (C_{Ar}), 129.95 (CH_{Ar}), 128.37 (CH_{Ar}), 128.26 (CH_{Ar}), 127.71 (CH_{Ar}), 127.47 (CH_{Ar}), 126.97 (CH_{Ar}), 126.61 (CH_{Ar}), 126.46 (CH_{Ar}), 121.59 (CH_{Ar}), 121.22 (CH_{Ar}), 114.75 (CH_{Ar}), 111.13 (CH_{Ar}), 55.14 (CH_{Ph2}), 52.19 (CH_3), 8.75 ($CH_{3\ imid}$), 6.74 ($CH_{3\ imid}$). Anal. calcd for $C_{45}H_{37}Cl_2N_3O_2Pd$ (829.13): C, 65.19; H, 4.50; N, 5.07. Found: C, 65.23; H, 4.27; N, 4.91.

General Procedure for the Synthesis of [Se(NHC)] Complexes. Selenium complex was synthesized according to a modified literature procedure.[24] A 7-mL screwcap vial equipped with a septum cap and a stirring bar was charged with imidazolium salt (3a) (0.16 g, 0.235 mmol, 1 equiv.), Se (0.02 g, 1.1 equiv.) and acetone (1 mL). The mixture was stirred at 40 °C for 15 min. NEt_3 (0.1 mL, 3 equiv.) was then added in one portion and the mixture was stirred overnight at 60 °C. Afterwards, the mixture was filtered through a plug silica gel and washed with DCM (20 mL). All volatiles were then removed under vacuum. The product was obtained as a yellow microcrystalline material.

[(IPr*^{Oxa})Se] (6a). The product was obtained in 77% yield (0.13 g, 0.18 mmol) as a yellow solid. Recrystallization from CH_2Cl_2/Et_2O at -20 °C gave suitable crystals for X-ray diffraction analysis. ^{1}H NMR (400 MHz, $CDCl_3$) δ 7.87 (d, *J* = 6.5 Hz, 1H, CH_{oxa}), 7.68 (d, *J* = 7.4 Hz, 1H, CH_{oxa}), 7.44 (t, *J* = 6.1 Hz, 2H, CH_{oxa}), 7.31 (d, *J* = 7.5 Hz, 4H, H_{Ar}), 7,21 - 7.18 (m, 8H, H_{Ar}), 7.14 (d, *J* = 5.9 Hz, 4H, H_{Ar}), 7.08 (d, *J* = 7.2 Hz, 4H, H_{Ar}), 6.84 (s, 2H, H_{Ar}), 5.39 (s, 2H, CH_{Ph2}), 2.22 (s, 3H, $CH_{3\ imid}$), 1.84 (s, 3H, $CH_{3\ imid}$), -0.09 (s, 3H, CH_3). ^{13}C NMR (101 MHz, $CDCl_3$) δ 160.23 (NCN), 151.45 (C_{Ar}), 150.70 (C_{oxa}), 143.13 (C_{Ar}), 143.10 (C_{Ar}), 140,80 (C_{Ar}), 140.66 (C_{Ar}), 139.50 (C_{oxa}), 132.15 (C_{Ar}), 130.52 (C_{Ar}), 130.09 (C_{Ar}), 129.79 (CH_{Ar}), 128.48 (CH_{Ar}), 128.26 (CH_{Ar}), 126.82 (CH_{Ar}), 126.49 (CH_{Ar}), 125.35 (CH_{Ar}), 123.60 (CH_{Ar}), 121.16 (CH_{Ar}), 111.62 (CH_{Ar}), 52.13 (CH_{Ph2}), 22.02 (CH_3), 9.35 ($CH_{3\ imid}$), 7.20 ($CH_{3\ imid}$). ^{77}Se NMR (95 MHz, $CDCl_3$) δ 119.41. Anal. calcd for $C_{45}H_{37}N_3OSe$ (714.77): C, 75.62; H, 5.22; N, 5.88. Found: C, 76.08; H, 5.06; N, 5.67.

General Procedure for the Synthesis of [Rh(NHC)(CO)Cl] Complexes. Rhodium complex was synthesized according to a modified literature procedure.[14g] Solid Rh(acac)$(CO)_2$ (0.05 g, 0.194 mmol) and imidazolium salt (3a) (0.05 g, 0.194 mmol) were weighed in a Schlenk tube in a glovebox. THF (10 mL) was then added, and the colour of the solution immediately turned yellow. After stirring for 2 h at room

temperature, the solvent was removed in vacuo, and the crude product was twice washed with Et_2O, giving the rhodium complex as a yellow solid.

[Rh(IPr*^{Oxa})(CO)Cl] (7a). The product was obtained in 57% yield (90 mg, 0.11 mmol) as a yellow solid. Recrystallization from CH_2Cl_2/Et_2O at RT gave suitable crystals for X-ray diffraction analysis. ^{1}H NMR (400 MHz, $CDCl_3$) δ 8.82 (d, *J* = 6.4 Hz, 1H, CH_{oxa}), 7.60 (s, 1H, CH_{oxa}), 7.45 (d, *J* = 29.6 Hz, 3H, $CH_{oxa,}$ CH_{Ar}), 7.19 (bs, 13H, H_{Ar}), 6.97 (d, *J* = 34.6 Hz, 8H, H_{Ar}), 5.56 (s, 2H, CH_{Ph2}), 2.24 (d, *J* = 29.9 Hz, 6H, $CH_{3\ imid}$), 0.01 (s, 3H). ^{13}C NMR (101 MHz, $CDCl_3$) δ 188.74 (Rh-CO), 183.45 (Rh-$C_{carbene}$), 158.28 (NCO), 149.58 (C_{oxa}), 142.08 (C_{Ar}), 141.97 (C_{Ar}), 140.86 (C_{Ar}), 140.32 (C_{oxa}), 137.74 (C_{Ar}), 132.34 (C_{Ar}), 131.29 (C_{Ar}), 130.29 (C_{Ar}), 129.77 (CH_{Ar}), 129.60 (CH_{Ar}), 128.44 (CH_{Ar}), 128.31 (CH_{Ar}), 127.04 (CH_{Ar}), 126.76 (CH_{Ar}), 126.63 (CH_{Ar}), 125.18 (CH_{Ar}), 121.02 (CH_{Ar}), 119.75 (CH_{Ar}), 110.56 (CH_{Ar}), 51.66 (CH_{Ph2}), 21.96 (CH_3), 9.06 ($CH_{3\ imid}$), 6.84 ($CH_{3\ imid}$). Anal. calcd for $C_{46}H_{37}ClN_3O_2Rh$ (802.18): C, 68.79; H, 4.77; N, 5.23. Found: C, 68.72; H, 4.56; N, 5.18. FT-IR (nujol): 1986 cm^{-1} ($\nu_{(C=O)}$).

General Procedure for the Three-Component Coupling Reaction. Previously reported procedure was followed.[25] Prepared according to the procedure using catalyst **4a** or **4b** (2 mol%), aldehyde (0.5 mmol), amine (0.55 mmol), alkyne (0.55 mmol) and MeOH (0.25 mL) at room temperature for 1 min. After the desired time, the conversion was determined by ^{1}H NMR or GC analysis. The mixture was diluted with Et_2O and filtered over a pad of silica.

1-(1-Cyclohexyl-3-phenyl-2-propynyl)piperidine. The product was obtained in 83% yield (116.80 mg, 0.5 mmol) as a yellow liquid. Purification by flash chromatography (petroleum ether/AcOEt = 10/1). ^{1}H NMR (400 MHz, $CDCl_3$) δ 7.45 – 7.42 (m, 2H), 7.31 – 7.24 (m, 3H), 3.10 (d, *J* = 9.9 Hz, 1H), 2.65 – 2.60 (m, 2H), 2.40 – 46 (m, 2H), 2.12 – 2.01 (m, 2H), 1.77 – 1.74 (m, 2H), 1.66 – 1.50 (m, 6H), 1.46 – 1.38 (m, 2H), 1.27 – 1,15 (m, 3H), 1.06 – 0.89 (m, 2H). ^{13}C NMR (101 MHz, $CDCl_3$) δ 131.87, 128.34, 127.76, 123.95, 87.94, 86.27, 64.54, 39.74, 31.50, 30.59, 26.97, 26.46, 26.27, 24.89.

General Procedure for the Heck Cross-Coupling Reaction. Previously reported procedure was followed.[14f] According to the procedure, catalyst **5a** or **5b** (0.2 mol%), base (1.50 mmol), and Bu_4NBr (0.2 mmol) were placed in a Schlenk tube containing a small stirring bar. The Schlenk tube was subjected to evacuation/backfilling cycles with argon, styrene (2.0 mmol), di(ethylene glycol) dibutyl ether (0.50 mmol), DMA (2.5 mL), and the haloarene (1.0 mmol) were added. The mixture was then heated at 135 °C for 2-24 h. After the desired time, the conversion was determined by ^{1}H NMR or GC analysis. The mixture was diluted with Et_2O and filtered over a pad of silica.

(*E*)-1-(4-Styrylphenyl)ethenone. The product was obtained in 98% yield (108.92 mg, 0.5 mmol) as a yellow liquid. Purification by flash chromatography (Hexane /AcOEt = 10/1). ^{1}H NMR (400 MHz, $CDCl_3$) δ 7.95 (d, *J* = 8.4 Hz, 2H), 7.59 (d, *J* = 8.3 Hz, 2H), 7.54 (d, *J* = 7.2 Hz, 2H), 7.38 (t, *J* = 7.5 Hz, 2H), 7.30 (t, *J* = 7.9 Hz, 1H), 7.21 (s, 1H), 7.13 (d, *J* = 16.4 Hz, 1H), 2.61 (s, 3H).^{13}C NMR (101 MHz, $CDCl_3$) δ 197.69, 142.16, 136.84, 136.08, 131.61, 129.05, 129.97, 128.49, 127.59, 126.98, 126.66, 76.88, 26.79.

(*E*)-1-Methoxy-4-styrylbenzene. The product was obtained in 91% yield (95.67 mg, 0.5 mmol) as a yellow liquid. Purification by flash chromatography (Hexane/ AcOEt = 10/1)**.** ^{1}H NMR (400 MHz, $CDCl_3$) δ 7.52 – 7.45 (m, 4H), 7.37 – 7.33 (m, 2H), 7.26 – 7.22 (m, 1H), 7.10 – 6.96 (m, 2H), 6.93 – 6.89 (m, 2H), 3.84 (s, 3H). ^{13}C NMR (101 MHz, $CDCl_3$) δ 159.46, 137.80, 130.30, 128.82, 128.37, 127.89, 127.39, 126.77, 126.42, 114.29, 55.51.

General Procedure for Hydrosilylation Reaction. Previously reported procedure was followed.[14f] According to the procedure, in a Schlenk tube, a solution of complex **7a** (0.005 mmol) in dry toluene (1.5 mL) was prepared, phenylacetylene (0.5 mmol), and triethylsilane (0.55 mmol), and *n*-dodecane (100 µL) were added in quick succession via syringe. The bright yellow reaction mixture was stirred at 100 °C for 24 h. The crude mixture was filtered through alumina and analyzed by GC-MS. The solvent was evaporated, the products were purified by flash chromatography through a short plug of silica and analyzed by ^{1}H NMR spectroscopy. The three reaction products were determined on the basis of the olefinic coupling constants in the ^{1}H NMR (400 MHz, $CDCl_3$) spectra: β-*(Z)*-isomer: 7.44 (d, *J* = 8.4 Hz), 5.76 (d, *J* = 15.2 Hz), β-(*E*)-isomer: 6.89 (d, *J* = 19.3 Hz), 6.43 (d, *J* = 19.3 Hz), α-isomer: 5.87 (d, *J* = 3.1 Hz), 5.57 (d, *J* = 3.1 Hz).

Conflicts of interest

There are no conflicts to declare.

Acknowledgements

We gratefully acknowledge Narodowe Centrum Nauki (grant no. 2019/35/D/ST4/00806), Rutgers University and the NSF (CAREER CHE-1650766) for generous financial support. We thank the Wroclaw Center for Networking and Supercomputing (grant number WCSS159).

Notes and references

1 a) D. Bourissou, O. Guerret, F. P. Gabbaï and G. Bertrand, *Chem. Rev.*, 2000, **100**, 39-92; For the original study by Arduengo, see: A. J. Arduengo III, R. L. Harlow, M. Kline, *J. Am. Chem. Soc.*, 1991, **113**, 361-363; c) A. J. Arduengo III, *Acc. Chem. Res.*, 1999, **32**, 913-921.

2 a) M. N. Hopkinson, C. Richter, M. Schedler and F. Glorius, *Nature*, 2014, **510**, 485-496; b) S. P. Nolan, *N-Heterocyclic Carbenes*, Wiley, 2014; c) S. Diez-Gonzalez, *N-Heterocyclic Carbenes: From Laboratory Curiosities to Efficient Synthetic Tools*, RSC, 2016; d) H. V. Huynh, *The Organometallic Chemistry of N-Heterocyclic Carbenes*, Wiley, 2017; e) C. S. J. Cazin, *N-Heterocyclic Carbenes in Transition Metal Catalysis*, Springer, 2011; f) E. A. B. Kantchev, C. J. O. O'Brien and M. G. Organ, *Angew. Chem. Int. Ed.*, 2007, **46**, 2768-2813; g) W. A. Hermann, *Angew. Chem. Int. Ed.*, 2002, **41**, 1290-1309; h) E. Peris, *Chem. Rev.*, 2018, **118**, 9988-10031; i) G. Sipos and R. Dorta, *Coord. Chem. Rev.*, 2018, **375**, 13-68; j) M. Iglesias and L. A. Oro, *Chem. Soc. Rev.*, 2018, **47**, 2772-2808; k) A. A. Danopoulos, T. Simler and P. Braunstein, *Chem. Rev.*, 2019, **119**, 3730-3961; l) Q. Zhao, G. Meng, S. P. Nolan and M. Szostak, *Chem. Rev.*, 2020, **120**, 1981-2048; m) C. Chen, F. S. Liu and M. Szostak, *Chem. Eur. J.*, 2021, **27**, 4478-4499; o) R. Jazzar, M. Soleilhavoup, and G. Bertrand, *Chem. Rev.*, 2020, **120**, 4141-4168; p) J. Morvan, M. Mauduit, G. Bertrand and R. Jazzar, *ACS Catal.*, 2021, **11**, 1714-1748; q) P. Gao and M. Szostak, Coord. *Chem. Rev.*, 2023, **485**, 215110.

3 a) D. J. Nelson and S. P. Nolan, *Chem. Soc. Rev.*, 2013, **42**, 6723-6753; b) S. Diez-Gonzalez and S. P. Nolan, *Coord. Chem. Rev.*, 2007, **251**, 874-883; c) H. Jacobsen, A. Correa, A. Poater, C. Costabile and L. Cavallo, *Coord. Chem. Rev.*, 2009, **253**, 687-703; d) T. Dröge and F. Glorius, *Angew. Chem. Int. Ed.*, 2010, **49**, 6940-6952.

4 a) H. Clavier and S. P. Nolan, *Chem. Commun.*, 2010, **46**, 841-861; b) A. Gomez-Suarez, D. J. Nelson and S. P. Nolan, *Chem. Commun.*, 2017, **53**, 2650-2660.

5 For an excellent review, see: H. V. Huynh, *Chem. Rev.* 2018, **118**, 9457-9492.

6 a) A. de Meijere, S. Bräse and M. Oestreich, *Metal-Catalyzed Cross-Coupling Reactions and More*, Wiley, 2014; b) G. A. Molander, J. P. Wolfe and M. Larhed, *Science of Synthesis: Cross-Coupling and Heck-Type Reactions*, Thieme, 2013; c) T. J. Colacot, *New Trends in Cross-Coupling: Theory and Applications*, RSC, 2015; d) G. C. Vougioukalakis and R. H. Grubbs, *Chem. Rev.*, 2010, **110**, 1746-1787; e) O. M. Ogba, N. C. Warner, D. J. O'Leary and R. H. Grubbs, *Chem. Soc. Rev.*, 2018, **47**, 4510-4544.

7 M. Koy, P. Bellotti, M. Das, and F. Glorius, *Nature Catal.*, 2021, **4**, 352-363.

8 a) K. M. Lee, C. K. Lee and I. J. B. Lin, *Angew. Chem. Int. Ed.*, 1997, **36**, 1850-1852; b) A. J. Boydston, K. A. Williams and C. W. Bielawski, *J. Am. Chem. Soc.*, 2005, **127**, 12496-12497; c) J. L. Hickey, R. A. Ruhayel, P. J. Barnard, M. V. Baker, S. J. Berners-Price and Filipovska, *J. Am. Chem. Soc.*, 2008, **130**, 12570-12571; d) K. M. Hindi, M. J. Panzner, C. A. Tessier, C. L. Cannon and W. J. Youngs, *Chem. Rev.*, 2009, **109**, 3859-3884; e) L. Mercs and M. Al-brecht, *Chem. Soc. Rev.*, 2010, **39**, 1903-1912; f) K. Oisaki, Q. Li, H. Furukawa, A. U. Czaja, and O. M. A. Yaghi, *J. Am. Chem.Soc.*, 2010, **132**, 9262-9264; g) K. V. S. Ranganath, J. Kloesges, A. H. Schafer and F. Glorius, *Angew. Chem. Int. Ed.*, 2010, **49**, 7786-7789; h) P. Lara, O. Rivada-Wheelaghan, S. Conejero, R. Poteau, K. Phillippot and B. Chaudret, *Angew. Chem. Int. Ed.*, 2011, **50**, 12080-12084;(i) A. V. Zhukhovitskiy, M. G. Mavros, T. V. Voorhis and J. A. Johnson, *J. Am. Chem. Soc.*, 2013, **135**, 7418-7421; j) R. Visbal and M. C. Gimeno, *Chem. Soc. Rev.*, 2014, **43**, 3551-3574.

9 a) O. Navarro, R. A. Kelly, III and S. P. Nolan, *J. Am. Chem. Soc.*, 2003, **125**, 16194-16195; b) N. Marion, O. Navarro, J. Mei, E. D. Stevens, N. M. Scott and S. P. Nolan, *J. Am. Chem. Soc.*, 2006, **128**, 4101-4111.

10 a) G. Altenhoff, R. Goddard, C. W. Lehmann and F. Glorius, *Angew. Chem. Int. Ed.*, 2003, **42**, 3690-3693; b) G. Altenhoff, R. Goddard, C. W. Lehmann and F. Glorius, *J. Am. Chem. Soc.*, 2004, **126**, 15195-15201; c) S. Würtz, C. Lohre, R. Fröhlich, K. Bergander and F. Glorius, *J. Am. Chem. Soc.*, 2009, **131**, 8344-8345.

11 a) V. Lavallo, Y. Canac, C. Präsang, B. Donnadieu and G. Bertrand, *Angew. Chem. Int. Ed.*, 2005, **44**, 5705; b) D. Martin, N. Lassauque, B. Donnadieu and G. Bertrand, *Angew. Chem. Int. Ed.*, 2012, **51**, 6172-6175; c) C. Weinstein, G. P. Junor, D. R. Tolentino, R. Jazzar, M. Melaimi and G. Bertrand, *J. Am. Chem. Soc.*, 2018, **140**, 9255-9260.

12 a) G. Berthon-Gelloz, M. A. Siegler, A. L. Spek, B. Tinant, J. N. H. Reek and I. E. Marko, *Dalton Trans.*, 2010, **39**, 1444-1446; b) F. Izquierdo, S. Manzini and S. P. Nolan, *Chem. Commun.*, 2014, **50**, 14926-14937.

13 a) T. Scatollin and S. P. Nolan, *Trends Chem.*, 2020, **2**, 721-736; b) Y. Wei, B. Rao, X. Cong and X. Zeng, *J. Am. Chem. Soc.*, 2015, **137**, 9250-9253; c) M. P. Wiesenfeldt, Z. Nairoukh, W. Li and F. Glorius, *Science*, 2017, **357**, 908-912; d) J. Diesel, A. Finogenova and N. Cramer, *J. Am. Chem. Soc.*, 2018, **140**, 4489-4493; e) S. Okumura, S. Tang, T. Saito, K. Semba, S. Sakaki and Y. Nakao, *J. Am. Chem. Soc.*, 2016, **138**, 14699-14704.

14 For selected examples, see: a) C. Fliedel, A. Labande, E. Manoury and R. Poli, *Coord. Chem. Rev.*, 2019, **394**, 65-193; b) S. Hemeury, P. de Fremont and P. Braunstein, *Chem. Soc. Rev.*, 2017, **46**, 632-733; c) A. Neshat, P. Mastrotilli and A. M. Mobarakeh, *Molecules*, 2022, **27**, 95; d) C. C. Tai, M. S. Yu, Y. L. Chen, W. H. Chuang, T. H. Lin, G. P. A. Yap and T. G. Ong, *Chem. Commun.*, 2014, **50**, 4344-4346; e) B. M. Zimmermann, T. T. Ngoc, D. I. Tzaras, T. Kaicharla and J. F. Teichert, *J. Am. Chem. Soc.*, 2021, **143**, 16865-17873; f) V. Cesar, S. Bellemin-Laponnaz, L. H. Gade, *Organometallics,* 2002, **21**, 5204-5208; g) M. Poyatos, A. Maisse-Francois, S. Bellemin-Laponnaz, L. H. Gade, *Organometallics* 2006, **25**, 2634-2641.

15 a) M. M. Rahman, G. Meng, E. Bisz, B. Dziuk, R. Lalancette, R. Szostak and M. Szostak, *Chem. Sci.*, 2023, **14**, 5141-5147; b) P. Gao, J. Xu, T. Zhou, Y. Liu, E. Bisz, B. Dziuk, R. Lalancette, R. Szostak, D. Zhang and M. Szostak, *Angew. Chem. Int. Ed.*, 2023, **62**, e202218427; c) J. Zhang, X. Li, T. Li, G. Zhang, K. Wan, Y. Ma, R. Fang. R. Szostak and M Szostak, *ACS Catal.*, 2022, **12**, 15323-15333; d) J. Zhang, Y. Wang, Y. Zhang, T. Liu, S. Fang, R. Wang, Y. Ma, R. Fang, R. Szostak, and M. Szostak, *Organometallics*, 2022, **41**, 1115-1124; e) Q. Xia, S. Shi, P. Gao, R. Lalancette, R. Szostak and M. Szostak, *J. Org. Chem.*, 2021, **86**, 15648-15657; f) P. Lei, Y. Wang, C. Zhang, Y. Hu, J. Feng, Z. Ma, X. Liu, R. Szostak and Szostak, *Org. Lett.*, 2022, **24**, 6310-6315; g) T. Zhou, S. Ma, F. Nahra, A. M. C. Obled, A. Poater, L. Cavallo, C. S. J. Cazin, S. P. Nolan and M. Szostak, *iScience*, 2020, **23**, 101377; h) S. Yang; T. Zhou, A. Poater, L. Cavallo, S. P. Nolan and M. Szostak, *Catl. Sci. Technol.*, 2021, **11**, 3189-3197; i) S. Yang, X. Yu and M. Szostak, *ACS Catal.*, 2023, **13**, 1848-1855; j) J. Zhang, T. Li, X. Li, A. Lv, X. Li, Z. Wang, R. Wang, Y. Ma, R. Fang, R. Szostak and M. Szostak, *Commun Chem.*, 2022, **5**, 60–70; k) M. M. Rahman, J. Zhang, Q. Zhao, J. Feliciano, E. Bisz, B. Dziuk, R. Lalancette, R. Szostak and M. Szostak, *Organometallics*, 2022, **41**, 2281-2290; l) J. Zhang, M. M. Rahman, Q. Zhao, J. Feliciano, E. Bisz, B. Dziuk, R. Lalancette, R. Szostak and M. Szostak, *Organometallics*, 2022, **41**, 1806-1815.

16 A. F. Cotton, G. Wilkinson, M. Bochmann, C. A. Murillo and M. Bochmann, Advanced Inorganic Chemistry, Wiley, 1999.

17 a) S. Meiries, K. Speck, D. B. Cordes, A. M. Z. Slawin, S. P. Nolan, *Organometallics*, 2013, **32**, 330-339; b) P. Zak, M. Bolt, J. Lorkowski, M. Kubicki and C. Pietraszuk, *ChemCatChem*, 2017, **9**, 3627-3631.

18 a) M. Szostak, Q. Zhao, and M. Rahman, US202163154948 March 1, **2021**; b) M. Kuriyama, N. Hamaguchi, G. Yano, K. Tsukuda, K. Sato, O. Onomura, *J. Org. Chem*., 2016, **81**, 8934-8946.

19 R. Visbal, A. Laguna, M. C. Gimeno, *Chem. Commun*., 2013, **49**, 5642-5644.

20 L. Falivene, Z. Cao, A. Petta, L. Serra, A. Poater, R. Oliva, V. Scarano and L. Cavallo, *Nat. Chem.*, 2019, **11**, 872-879.

21 P. De Fremont, N. M. Scott, E. D. Stevens, T. Ramnial, O. C. Lightbody, C. L. B. Macdonald, J. A. C. Clyburne, C. D. Abernethy and S. P. Nolan, *Organometallics*, 2005, **24**, 6301-6309.

22 a) S. V. C. Vummaleti, D. J. Nelson, A. Poater, A. Gomez-Suarez, D. B. Cordes, A. M. Z. Slawin, S. P. Nolan and L. Cavallo, *Chem. Sci.*, 2015, **6**, 1895-1904; b) A. Liske, K. Verlinden, H. Buhl, K. Schaper and C. Ganter, *Organometallics*, 2013, **32**, 5269-5272; c) G. P. Junor, J. Lorkowski, C. M. Weinstein, R. Jazzar, C. Pietraszuk and G. Bertrand, *Angew. Chem. Int. Ed.*, 2020, **59**, 22028-22033.

23 K. Azouzi, C. Duhayon, I. Benaissa, N. Lugan, Y. Canac, S. Bastin and V. Cesar, *Orgnaometallics*, 2018, **37**, 4726-4735.

24 S. P. Nolan, N. Tzouras, F. Nahra, L. Falivene, L. Cavallo, M. Saab, M. Cazin, *Chem. Eur. J.,* 2020, **20***,* 4515–4519.

25 a) M. T. Chen, B. Landers, O. Navarro, *Org. Biomol. Chem*., 2012, **10**, 2206–2208; b) Z. Wang, N. V. Tzouras, S. P. Nolan and X. Bi, *Trends Chem.,* 2021, **3**, 674–685; c) S. Yang, T. Zhou, X. Yu and M. Szostak, *Molecules*, 2023, **22**, 1672.

26 J. P. Morales-Ceron, P. Lara, J. Lopez-Serrano, L. L. Santos, V. Salazar, E. Alvarez and A. Suarez, *Organometallics,* 2017, **36**, 2460-2469.